DOI: 10.1002/ejic.200900549

Structural and Near-IR Luminescent Properties of Erbium-Containing Coordination Polymers

Victor Haquin,[a] Frédéric Gumy,[b] Carole Daiguebonne,*[a] Jean-Claude Bünzli,*[b] and Olivier Guillou[a]

Keywords: Heterometallic complexes / Lanthanides / X-ray diffraction / Luminescence / Polymers

The near-IR luminescence properties of two Er^{III}-containing coordination polymers, namely, $[Er(btc)(H_2O)_5{\cdot}3.5H_2O]_\infty$ [$(btc)^{3-}$ = 1,3,5-benzenetricarboxylate] and $[Er_2(bdc)_3(H_2O)_4]_\infty$ [$(bdc)^{2-}$ = 1,4-benzenedicarboxylate] were investigated with the aim of testing their potential use as optical materials. Because both present relatively small quantum yields and short excited-state lifetimes, factors influencing their luminescent properties were deciphered in an effort to improve their luminescent properties. Thus, three other families of compounds were also investigated: (i) the two corresponding dehydrated compounds with respective chemical formula [Er(btc)] and $[Er_2(bdc)_3]_\infty$ for evaluating the importance of O–H vibrators, (ii) the heterodinuclear compounds $[Er_{2-2x}Y_{2x}(bdc)_3(H_2O)_4]_\infty$ (x = 0.2, 0.5, 0.8 and 0.9) for estimating the role of intermetallic quenching and (iii) the heterodinuclear compounds $[Er_{2-2x}Yb_{2x}(bdc)_3(H_2O)_4]_\infty$ (x = 0.2 and 0.5) for checking whether Yb^{III}-sensitized up-conversion can be induced or not.

Introduction

Historically, interest in the near-infrared (NIR) emission properties of lanthanide ions has been strengthened by the development of optical fibres and laser amplifiers used for long-distance telecommunication.[1–3] Actually, the Er^{III} ion exhibits a 4f intrashell transition from its first excited state $^4I_{13/2}$ to the ground state $^4I_{15/2}$, which occurs at a wavelength of 1540 nm. Optical 4f intrashell transitions are partially forbidden in the free Er^{III} ion. However, when incorporated into solid hosts, the crystal field of the host induces a mixing of states, thus relaxing the selection rules. In matrices devoid of high-energy vibrations, particularly OH or NH, but also CH,[4] the Er($^4I_{13/2}$) lifetime is in the millisecond range and may even reach 24 ms.[5] This makes Er-doped materials attractive for laser and optical amplifiers operating at 1540 nm, which is one of the standard telecommunication wavelengths. Initially, these devices have mostly implied purely inorganic compounds such as silica, alumina or $LiNbO_3$ or nonoxide glasses as host matrix.[6–9] Since the discovery of electroluminescence in poly(*para*-phenylenevinylene)[10] lanthanide complexes, organic ligands have been doped into various polymers in attempts to produce cheaper and more versatile optical materials for telecommunications and light-emitting diodes.[11] Metal–organic infinite frameworks containing luminescent lanthanide ions connected by multifunctional organic ligands[3] may constitute an alternative approach for designing such devices. Indeed, some of the drawbacks encountered with the doped condensed phases or glasses can be avoided with these metal–organic frameworks. For instance, the spatial distribution of the lanthanide ions is perfectly controlled in coordination polymers, and compounds with as much as 50 wt.-% of lanthanide ions can be designed. However, although the number of reported luminescent lanthanide-containing coordination polymers is steadily increasing,[12] relatively few of them have been specifically designed for emission in the NIR[13–15] and quantitative data are scarce.[11] In order to evaluate the potential interest of Er-containing coordination polymers for optical applications, we present here a study of two Er^{III}-containing coordination polymers, namely, $\{[Er(btc)(H_2O)_5]{\cdot}3.5H_2O\}_\infty$ [btc^{3-} = 1,3,5-benzenetricarboxylate $(C_9H_3O_6)^{3-}$, hereafter referred as **1**-Er], and $[Er_2(bdc)_3(H_2O)_4]_\infty$ [bdc^{2-} = 1,4-benzenedicarboxylate $(C_8H_4O_4)^{2-}$, hereafter referred as **2**-Er]. The structures of the ligands are given in Figure 1.

The crystal structures of both compounds are known: $\{[Er(btc)(H_2O)_5]{\cdot}3.5H_2O\}_\infty$ (**1**-Er) consists in the juxtaposition of neutral 1D chain-like molecular motifs[16] (Figure 2), whereas $[Er_2(bdc)_3(H_2O)_4]_\infty$ is 3D[17] (Figure 3). There are two Er^{III} ions per unit cell in $\{[Er(btc)(H_2O)_5]{\cdot}3.5H_2O\}_\infty$, that is, 2.5 Er^{III} ions per 1000 Å^3 or 2.5×10^{21} ions cm^{-3}, and eight Er^{III} ions per unit cell in $[Er_2(bdc)_3(H_2O)_4]_\infty$, representing 3.35 Er^{III} ion per 1000 Å^3. Moreover, there are five coordination water molecules and three and a half crystallization water molecules per erbium

[a] Institut National des Sciences Appliquées, UMR 6226 "Sciences Chimiques de Rennes", 35043 Rennes
E-mail: carole.daiguebonne@insa-rennes.fr
[b] École Polytechnique Fédérale de Lausanne – Laboratoire de Chimie Supramoléculaire des Lanthanides, BCH 1402, 1015 Lausanne, Switzerland

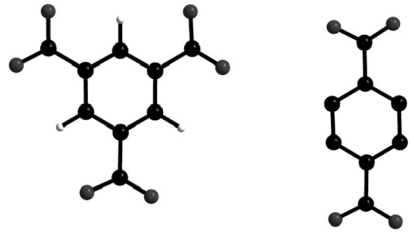

Figure 1. Schematic representation of the $(btc)^{3-}$ (left) and $(bdc)^{2-}$ (right) ligands.

ion in the latter, whereas there are only two coordination molecules and no crystallization water molecules in the former. Finally, as shown in Table 1, the intermetallic distances are substantially different in the two structures.

Table 1. Ten shortest intermetallic distances in **1**-Er and **2**-Er crystal structures.[a]

1-Er		**2**-Er	
Symmetry code	Er–Er / Å	Symmetry code	Er–Er / Å
0.5 – *x*, –0.5 + *y*, 0.5 – *z*	8.517	1 + *x*, *y*, *z*	6.142
–*x*, –*y*, –*z*	9.901	–1 –*x*, –1 – *y*, –1 – *z*	5.093
–0.5 + *x*, 0.5 – *y*, –0.5 + *z*	7.556	–1 – *x*, –1 – *y*, –*z*	5.025
–*x*, *y*, 0.5 – *z*	6.928	–1 + *x*, *y*, *z*	6.142
–0.5 + *x*, –0.5 + *y*, *z*	11.245	–2 – *x*, –1 – *y*, –1 – *z*	7.824
0.5 – *x*, 0.5 – *y*, –*z*	7.225	–*x*, –1 – *y*, –1 – *z*	8.131
x, –*y*, –0.5 + *z*	10.175	–*x*, –1 – *y*, –*z*	7.938
–*x*, 1 –*y*, –*z*	11.973	–2 – *x*, –1 – *y*, –*z*	7.934
–0.5 + *x*, 0.5 + *y*, *z*	11.245	2 + *x*, *y*, *z*	12.284
x, 1 – *y*, 0.5 + *z*	12.200	–2 + *x*, *y*, *z*	12.284

[a] For both crystal structures all distances are relative to the erbium atom with (*x*, *y*, *z*) symmetry code.

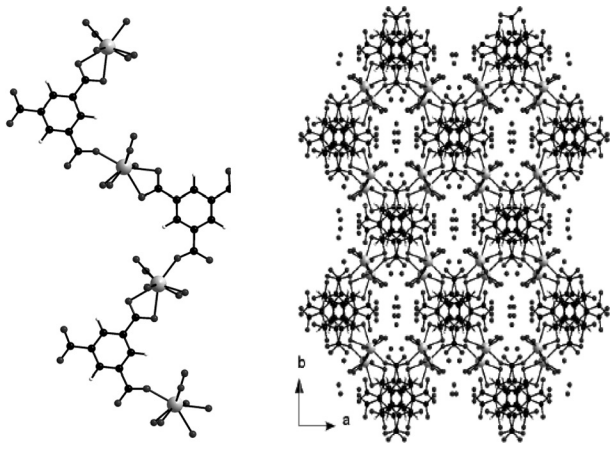

Figure 2. Projection view of a molecular motif of $\{[Er(btc)(H_2O)_5]\cdot 3.5H_2O\}_\infty$ (left); projection view along the *c* axis of the crystal packing (right). $\{[Er(btc)(H_2O)_5]\cdot 3.5H_2O\}_\infty$ crystallizes in the monoclinic system, space group *C*2/*c* (n°15) with a = 147396(15) Å, b = 16.9874(15) Å, c = 14.4591(14) Å, β = 118.754(9)°, V = 3174(1) Å^3 and Z = 8.

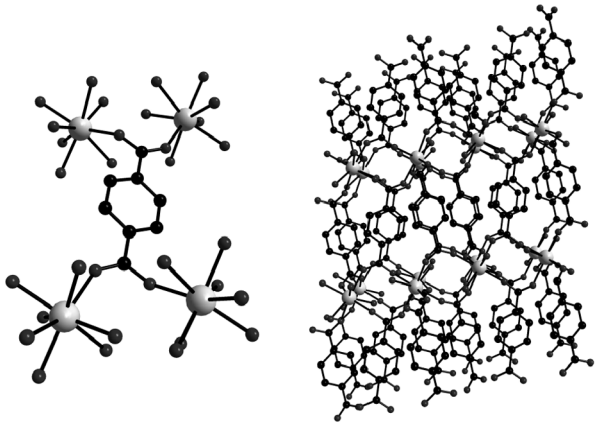

Figure 3. Perspective views of an extended unit cell of $[Er_2(bdc)_3(H_2O)_4]_\infty$ (left) and of the crystal packing (right). $[Er_2(bdc)_3(H_2O)_4]_\infty$ crystallizes in the triclinic system, space group $P\bar{1}$ (n°2) with a = 6.153(3) Å, b = 10.008(6) Å, c = 10.035(4) Å, α = 102.03(3)°, β = 91.61(3)°, γ = 101.20(4)°, V = 591.4(3) Å^3 and Z = 2.

It is well established that hydration and/or intermetallic distances play an important role in luminescent properties and that the number of Er^{III} ions per unit volume is a key parameter in waveguide amplifiers. All these reasons led us to select **1**-Er and **2**-Er for investigating the effects of these parameters and for testing their interest for NIR-luminescent materials.

Results and Discussion

The emission spectra of **1**-Er and **2**-Er recorded under direct excitation into the Er($^4F_{7/2}$) level at 488 nm and at both 295 and 10 K are depicted on Figure 4 (top). The corresponding excitation spectra recorded for deuterated compounds **1**-Er(D_2O) and **2**-Er(D_2O) are shown at the bottom of Figure 4. They feature both f–f transitions and a broad band from the ligand, pointing to some ligand-to-metal energy transfer in these compounds.

For the two investigated compounds, the characteristic Er($^4I_{13/2}\rightarrow{}^4I_{15/2}$) transition in the NIR region appears as a broad band with full-width-at-half-maximum (fwhm) of about 70 (**1**-Er) and 40 nm (**2**-Er) at 295 K, another interesting feature of these compounds with respect to potential optical applications. The emission of **2**-Er is more intense compared to that of **1**-Er, as may be inferred from the signal-to-noise ratios seen in Figure 4. At low temperature, the lines are narrower and crystal-field components are clearly evidenced, in particular for $[Er_2(bdc)_3(H_2O)_4]_\infty$. In the latter case, eight major and two to three minor components are identified; because the maximum splitting of $^4I_{15/2}$ in low-symmetry crystal field is eight, this means that the chemical environments of the Er^{III} ions are reasonably homogeneous. The lifetime of the Er($^4I_{13/2}$) excited state is ca. 1 μs for **1**-Er and less than 0.1 μs (the limit of our apparatus) for **2**-Er (Table 2). The overall quantum yield of **2**-Er was estimated according to Wrigthon's method[18] to Q^L_{Er} = 0.0013%, a value which increases by a factor of 10 upon deuteration of the sample in **2**-Er(D_2O). In contrast, the emissions of both **1**-Er and **1**-Er(D_2O) are too low in intensity to obtain reliable quantum yield data.

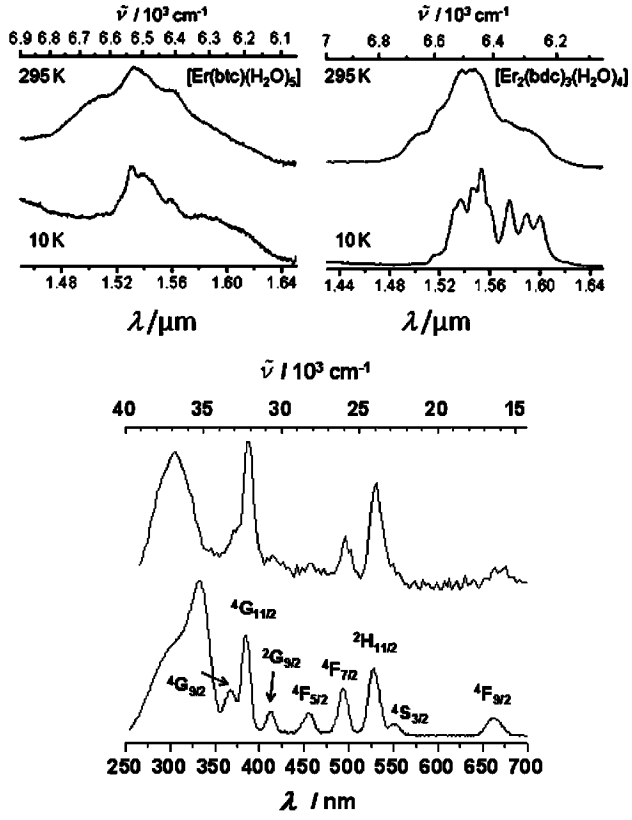

Figure 4. Top: $^4I_{13/2} \rightarrow {}^4I_{15/2}$ transition for compounds **1**-Er (left) and **2**-Er (right); λ_{exc} = 488 nm; bottom: excitation spectra of **1**-Er(D_2O) and **2**-Er(D_2O) at 295 K (λ_{an} = 1.54 μm).

Table 2. Photophysical data for the investigated compounds.[a]

Compound	$\tau_{295\,K}$ / μs	$\tau_{10\,K}$ / μs	$10^4 Q^L_{Ln}$ (295 K)
1-Er	<0.1	<0.1	–[b]
1-Er(D_2O)	0.64(1)	0.89(1)	–[b]
[Er(btc)]	1.0(1)	2.3(1)	0.45(2)
2-Er	<0.1	n.a.	≈0.13
2-Er(D_2O)	2.50(1)	2.80(1)	1.3(6)
$[Er_2(bdc)_3]_\infty$	4.91(4)	5.01(4)	2.2(1)

[a] Standard deviations (2σ) between parentheses; λ_{exc} = 355 nm (τ) or 305 nm (Q). [b] Too weak to be measured.

These very-low quantum yields are not surprising, because both compounds contain several coordination or crystallization water molecules, and O–H vibrators are very efficient inhibitors of NIR luminescence. We have thus thermally dehydrated these compounds. As shown previously,[17,19–21] dehydration of **1**-Er provokes the collapse of the molecular framework and leads to a quasiamorphous phase with chemical formula [Er(btc)] that reversibly binds water to reform **1**-Er. Despite great efforts, this phase has not yet been structurally characterized. In contrast, dehydration of 3D **2**-Er leads to a well-crystallized phase with chemical formula $[Er_2(bdc)_3]_\infty$ that has been previously structurally characterized[17,22] (Figure 5).

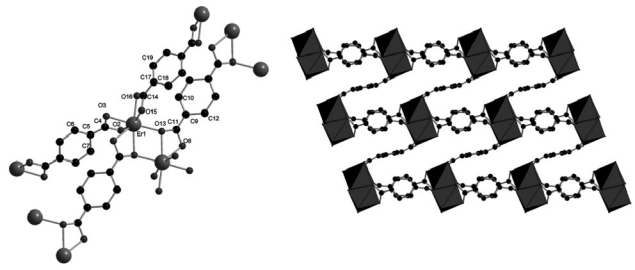

Figure 5. Left: Projection view along with numbering scheme of an extended asymmetric unit of $[Er_2(bdc)_3]_\infty$; right: perspective view along the c axis of $[Er_2(bdc)_3]_\infty$. Er coordination polyhedra are drawn. $[Er_2(bdc)_3]_\infty$ crystallizes in the triclinic system, space group $P\bar{1}$ (n°2) with a = 10.1508(8) Å, b = 8.9181(6) Å, c = 7.4031(5) Å, α = 106.749(4)°, β = 98.832(5)°, γ = 107.279(5)°, V = 591 Å^3 and Z = 2.

The luminescence spectra of both dehydrated compounds are presented on Figure 6. They are in line with the structural properties. For instance, [Er(btc)] gives rise to a broad spectrum at 295 K (fwhm = 45 nm), which does not resolve into sharp crystal-field components at 10 K and thus is characteristic of an amorphous material. In contrast, although the emission of $[Er_2(bdc)_3]$ remains broad at 295 K (fwhh ≈ 40 nm), it displays eight sharp transitions in the range 1.52–1.57 μm, reflecting a compound with high crystallinity and with one chemical environment for Er^{III}. We tentatively assign the three bands in the range 1.62–1.64 μm to crystal-field components of the $^4S_{3/2} \rightarrow {}^4I_{9/2}$ transition. The lifetimes of the Er($^4I_{13/2}$) level in [Er(btc)] is about 10 times longer than that of the hydrated compound (Table 2) and even reaches 2.27(3) μs at 10 K; the quantum yield is now measurable, Q^L_{Er} = 0.0045(2)%. This is still very low, but as expected, dehydration has substantially increased the luminescence properties of the compound. For $[Er_2(bdc)_3]_\infty$, the overall quantum yield is 17-fold larger than that for the analogous hydrated compound **2**-Er and well in the range of reported values for erbium complexes with organic ligands, 0.01–0.03%.[11] Because the Er^{III} content is similar in both hydrated (3.35 Er/1000 Å^3) and dehydrated (3.40 Er/1000 Å^3) compounds the improvement in photophysical properties upon dehydration is solely due to removal of the quenching water molecules. On the basis of these results, we decided to concentrate further investigations on **2**-Er because it is more promising than **1**-Er.

Another phenomenon can be responsible of a weak quantum yield is the so-called intermetallic quenching. It is generally admitted that the closer to each other the metallic centres are, the more efficient this phenomenon is.[23,24] Coordination polymer **2**-Er belongs to a recently described[25] wide family of isostructural compounds with general chemical formula $[(\sum_{i=1}^{13} \ln_x{}^i)(C_8H_4O_4)_3(H_2O)_4]_\infty$ with $\sum_{i=1}^{13} x_i = 2$ and in which Ln^i represents one of the lanthanide ions comprised between La and Tm (except Pm) or Y[38] Therefore, we synthesized several heterodinuclear compounds with general chemical formula $[Er_{2-2x}Y_{2x}(bdc)_3{\cdot}4H_2O]_\infty$ with $0 \leq x \leq 1$. All these compounds are isostructural to **2**-Er

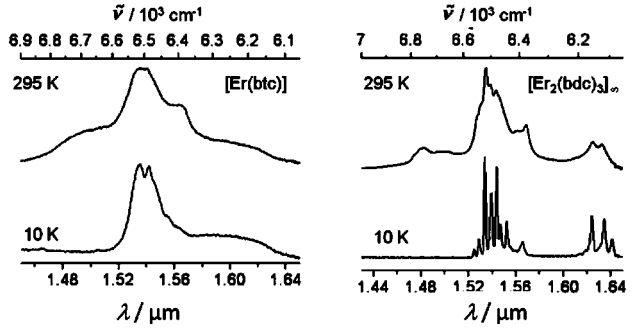

Figure 6. $^4I_{13/2} \rightarrow {}^4I_{15/2}$ transition for compounds [Er(btc)] (left) and $[Er_2(bdc)_3]_\infty$ (right); λ_{exc} = 488 nm.

and are hereafter referred as **2**-$Er_{2-2x}Y_{2x}$. In these compounds, the Y^{III} and Er^{III} ions are randomly distributed over the metallic centres of the crystal structure. There is neither segregation nor order and each metallic centre is structurally best described by a fictive atom $Er_{2-2x}Y_{2x}$. Y^{III} ions are optically inactive and their introduction produces only a dilution of the Er^{III} ions.

In **2**-Er, a given Er^{III} ion is surrounded by 26 other Er^{III} ions, as shown in Figure 7. The average of these 26 distances (d_{Er} = 10.3 Å) was assumed to be a good estimation of the mean distance between two erbium ions. In the frame of this assumption, the mean distance between two erbium ions in compound **2**-$Er_{2-2x}Y_{2x}$ is: $d_{Er_{1-x}Y_x} = d_{Er}/(1 - x)$ (Table 3).

The emission spectra of compound **2**-$Er_{2-2x}Y_{2x}$ (x = 0, 0.2, 0.5, 0.8 and 0.9) were measured (Figure 8). Unfortunately, the small emission intensities do not allow the determination of lifetimes of the excited states nor quantum yields. However, from Figure 8, it is apparent that the luminescence intensity does not significantly vary from one compound to another. This suggests that the dilution of the Er^{III} ions improves their luminescence. Actually, the luminescence intensity remains unchanged, whereas the Er^{III} content is reduced by a factor of five.

Because the NIR luminescence of Er^{III}-containing systems can be improved by sensitization through Yb^{III}, we synthesized compounds with general chemical formula $[Er_{2-2x}Yb_{2x}(bdc)_3(H_2O)_4]_\infty$. X-ray diffraction diagrams of several samples with x varying between 0 and 1 are presented in Figure 9. From this figure it is clear that compounds with general chemical formula $[Er_{2-2x}Yb_{2x}(bdc)_3(H_2O)_4]_\infty$ are obtained for $0 \leq x \leq 0.8$ and compounds with formula $\{[Er_{2-2x}Yb_{2x}(bdc)_3(H_2O)_8]\cdot 2H_2O\}_\infty$ are obtained for $0.9 \leq x \leq 1.0$, much as when reacting Yb^{III} with $(bdc)^{3-}$ (x = 1).[21] $[Yb_2(bdc)_3(H_2O)_8\cdot 2H_2O]_\infty$ crystallizes in the triclinic system, space group $P\bar{1}$ (n°2) with a = 7.539(1) Å, b = 10.0533(3) Å, c = 10.04578(3) Å, α = 87.7870(10)°, β = 82.5510(11)°, γ = 86.2800(16)°, Z = 2 and V = 783.92(4) Å^3. For x values between 0.8 and 0.9, different situations were encountered and it was not possible to find any rationalization (Figure 10). In this "rule-less" field, some microcrystalline powders have been identified, for example, $[Er_{2-2x}Yb_{2x}(bdc)_3(H_2O)_4]_\infty$, $[Er_{2-2x}Yb_{2x}(bdc)_3$-

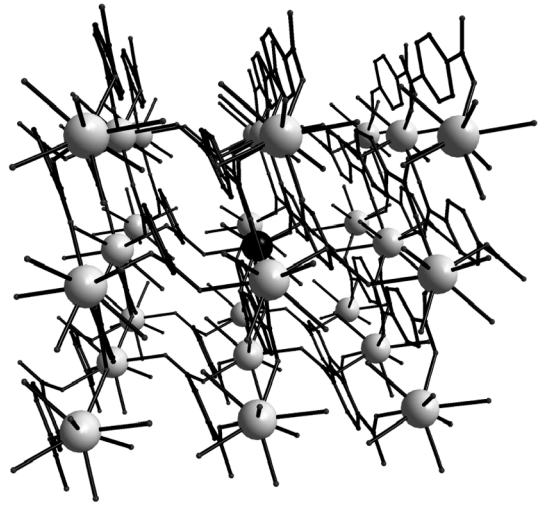

Figure 7. Perspective view along the b axis of a central Er atom with symmetry code (x, y, z, black spheres) and its 26 surrounding Er atoms (grey spheres). The Er–Er distances relative to the central atom are listed hereafter: Distance [Å] (symmetry code): 6.142 (–1 + x, y, z); 6.142 (1 + x, y, z); 7.938 (–x, –1 – y, –z); 5.025 (–1 – x, –1 – y, –z); 7.934 (–2 – x, –1 – y, –z); 8.131 (–x, –1 – y, –1 – z); 5.093 (–1 – x, –1 – y, –1 – z); 7.824 (–2 – x, –1 – y, –1 – z); 13.308 (–x, –2 – y, –1 – z); 10.594 (–1 – x, –2 – y, –1 – z); 11.081 (–2 – x, –2 – y, –1 – z); 12.799 (1 + x, –1 + y, z); 10.069 (x, –1 + y, z); 10.697 (–1 + x, –1 + y, z); 14.735 (–x, –2 – y, –z); 12.436 (–1 – x, –2 – y, –z); 12.948 (–2 – x, –2 – y, –z); 10.568 (–x, –y, –z); 9.931 (–1 – x, –y, –z); 12.689 (–2 – x, –y, –z); 10.697 (1 + x, 1 + y, z); 10.069 (x, 1 + y, z); 12.799 (–1 + x, 1 + y, z); 12.567 (–x, –y, –1 – z); 11.935 (–1 – x, –y, –1 – z); 14.227 (–2 – x, –y, –1 – z).

Table 3. Characteristic structural parameters of several compounds **2**-$Er_{2-x}Y_{2x}$ with $0 \leq x \leq 1$.

Compound	x	Er/1000 Å^{-3}	$d_{Er_{1-x}Y_x}$ / Å
2-Er	0.0	3.35	10.3
2-$Er_{0.8}Y_{0.2}$	0.2	2.68	12.9
2-$Er_{0.5}Y_{0.5}$	0.5	1.67	20.6
2-$Er_{0.2}Y_{0.8}$	0.8	0.67	51.5
2-$Er_{0.1}Y_{0.9}$	0.9	0.33	103.0
2-Y	1.0	0.00	–

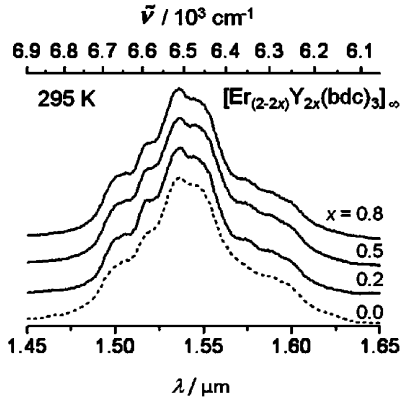

Figure 8. Luminescent spectra at 295 K of **2**-$Er_{2-2x}Y_{2x}$ (x = 0, 0.2, 0.5 and 0.8).

$(H_2O)_8{\cdot}2H_2O]_\infty$, $[Er_{2-2x}Yb_{2x}(bdc)_3(H_2O)_6]_\infty$[21,26,39] or mixtures of these phases. This illustrates the great versatility of the terephthalate/lanthanide system.

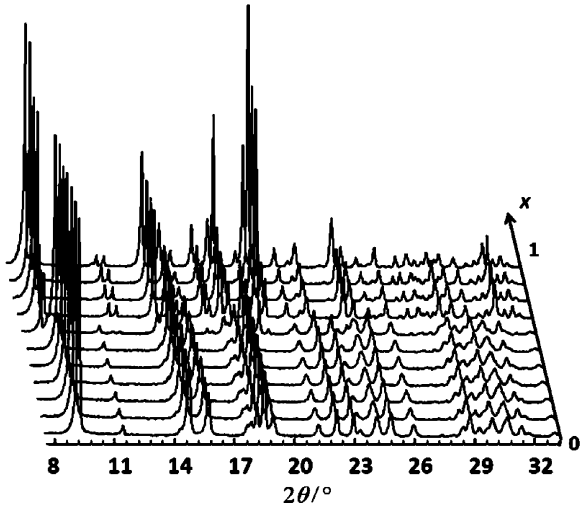

Figure 9. X-ray diffraction diagrams of Yb/Er-containing heterodinuclear compounds.

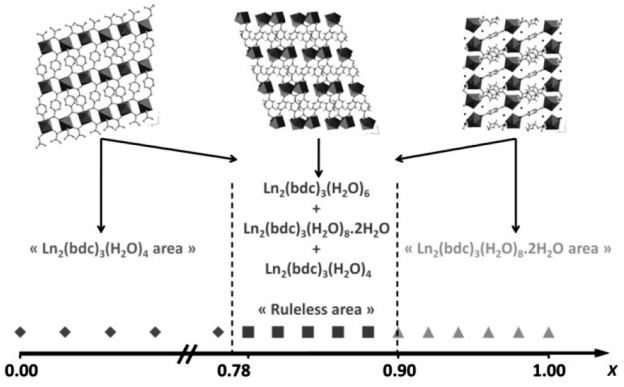

Figure 10. Structural types of the microcrystalline powders vs. x. The symbols on the bottom of the figure symbolize the analyzed microcrystalline powders.

Samples obtained for $0 \leq x \leq 0.8$ were analyzed in detail by X-ray diffraction, elemental analysis and SEM measurements according to a procedure previously described.[25] This analysis clearly shows that they are monophasic and have the expected chemical formula and structural type. This result confirms the large stability of this structural type.

The luminescence spectra of $[Er_{2-2x}Yb_{2x}(bdc)_3(H_2O)_4]_\infty$ compounds (x = 0, 0.2 and 0.5) are reported in Figure 11. The three spectra are almost identical. Comparison between luminescence spectra of homologous compounds $[Er_{2-2x}Ln_{2x}(bdc)_3(H_2O)_4]_\infty$ with Ln = Y and Yb seems to indicate that Yb^{III} ions and Y^{III} ions play a similar role when the compounds are excited in the ligand levels: they act as spacers and no improved sensitization by transfer through Yb^{III} is observed up to x = 0.5 when Yb^{III} ions are involved. Above x = 0.5, the overall shape of the emission band changes substantially, indicating a structural change.

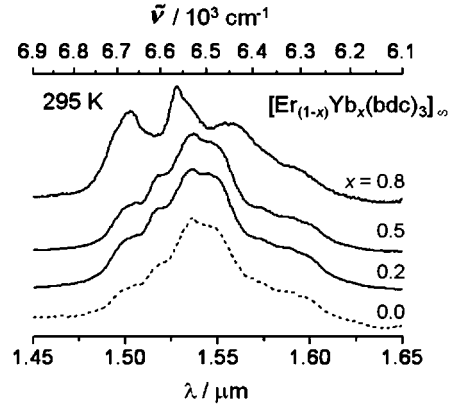

Figure 11. Luminescence spectra measured for $[Er_{2-2x}Yb_{2x}(bdc)_3(H_2O)_4]_\infty$ (x = 0, 0.2, 0.5 and 0.8).

Conclusions

The potential interest of Er^{III}-containing coordination polymers based on di- and tricarboxylates was evaluated with respect to their NIR luminescence. The latter is largely enhanced upon dehydration of the initial $\{[Er(btc)(H_2O)_5]\cdot 3.5H_2O\}_\infty$ and $[Er_2(bdc)_3(H_2O)_4]_\infty$ coordination polymers, and the quantum yield of $[Er_2(bdc)_3]_\infty$ reaches a value in the range of those previously reported for complexes with organic ligands. An interesting point lies in the fact that Er^{III} can be diluted by Y^{III} in a proportion to 1:5 without apparent loss of emission intensity. However, the presence of C–H oscillators is the main weakness of these organic–inorganic hybrid materials, which are still far from the performances displayed by inorganic clusters such as $(thf)_{14}Er_{10}S_6(Se_2)_6I_6$,[27] which presents a lifetime as long as 3 ms and an intrinsic quantum yield of 78%, $Q^{Er}_{Er} = \tau_{obs}/\tau^{rad} = Q^{L}_{Ln}/\eta_{sens}$, where η_{sens} is the efficacy with which the ligands transfer energy onto the metal ion. In our case, the intrinsic quantum yield is only about 0.4% (taking τ^{rad} = 12 ms). However, in view of the advantages that coordination polymers could present, particularly with respect to their introduction into nanoparticles,[17] we are now pursuing the project by trying to obtain such Er^{III}-containing coordination polymers devoid of C–H vibrations, namely, by replacing C–H bonds with C–F or C–Cl bonds.

Experimental Section

Synthesis: Terephthalic acid $H_2(bdc)$ and trimesic acid $H_3(btc)$ were purchased from Acros Organics and used without further purification. Sodium terephthalate (or trimesate) salt was prepared by addition of 2 equivalents (or 3 equiv.) of sodium hydroxide to a suspension of terephthalic (or trimesic) acid in deionized water. The obtained solution was then evaporated to dryness. The resulting solid was suspended in ethanol, and the mixture was stirred at reflux for 1 h. After filtration and drying, a white powder of disodium 1,4-benzenedicarboxylate (or trisodium 1,3,5-benzenetricarboxylate) was collected in 90% yield. $C_8H_4Na_2O_4$ (210.10): calcd. C 45.7, H 1.9, Na 21.9, O 30.5; found C 45.5, H 2.0, Na 22.0, O 30.5 [or $C_9H_3O_6Na_3$ (276.09): calcd. C 39.2, H 1.1, Na 25.0, O 34.8; found C 39.1, H 1.0, Na 25.3, O 34.5.

Hydrated lanthanide chlorides were prepared from the corresponding oxides according to literature methods.[28] Lanthanide oxides were purchased from Strem Chemicals and used without further purification.

Microcrystalline powders of the coordination polymers were obtained by mixing at room temperature stoichiometric amounts of mixtures of lanthanide chlorides in water with the sodium salt of terephthalic (respectively trimesic) acid. Precipitation immediately occurred. The white precipitates were filtered and dried in air. The yields of the reactions were close to 100%. FTIR spectra show the expected strong characteristic absorptions for the symmetric and asymmetric vibrations of benzenedi(tri)carboxylate ligands (1650–1550 cm^{-1} and 1420–1335 cm^{-1}) and the coordinated water molecules (3460 cm^{-1}). They show no absorption band of any protonated ligand (1715–1680 cm^{-1}). $[Er(btc)(H_2O)_5{\cdot}3.5H_2O]_\infty$ (524.48): calcd. C 20.6, H 3.3, Er 31.9, O 44.2; found C 20.5, H 3.2, Er 31.8, O 44.5. $[Er_2(bdc)_3(H_2O)_4]_\infty$ (898.926): calcd. C 32.1, H 2.2, O 28.5, Er 37.2; found C 32.0, H 2.0, Er 37.5, O 28.5. $[Y_2(bdc)_3(H_2O)_4]_\infty$ (742.22): calcd. C 38.8, H 2.7, O 34.5, Y 24.0; found C 38.5, H 3.0, O 34.5, Y 24.0). $[Yb_2(bdc)_3(H_2O)_8{\cdot}2H_2O]_\infty$ (1018.58): calcd. C 28.3, H 3.2, O 34.6, Yb 34.0; found C 28.5, H 3.2, O 34.5, Y 33.9.

The results of the elemental analysis of the heterodinuclear coordination polymers are summarized in Tables 4 and 5. Deuterated compounds **1**-Er(D_2O) and **2**-Er(D_2O) were obtained from the anhydrous complexes [Er(btc)] and $[Er(bdc)_3]_\infty$, which were suspended in D_2O and stirred for 20 min. The resulting solids were filtered, washed with [D_6]acetone and left to dry overnight. All operations were carried out in a glove-box with nitrogen atmosphere.

The obtained microcrystalline powders were all assumed to be respectively isostructural to the previously described compounds $[Er(btc)(H_2O)_5{\cdot}3.5H_2O]_\infty$,[16] $[Er_2(bdc)_3(H_2O)_4]_\infty$ or $[Er_2(bdc)_3(H_2O)_8{\cdot}2H_2O]_\infty$[21] on the basis of their X-ray powder diffraction diagrams. The homogeneity of the heterodinuclear samples was checked by SEM measurements. The results confirm that all the particles forming the microcrystalline powders have the same chemical formula than the powders.

The monophasic character of the heterodinuclear compounds was established on the basis of their X-ray diffraction diagrams. The diffraction peaks on the diffraction diagram of the heterodinuclear compounds show no splitting. Furthermore, there are neither additional peaks (characteristic of a superstructure) nor broadening of the peaks (characteristic of disorder). This indicates that, in these heterobinuclear compounds, there is no order or segregation: In these compounds, the metallic ions are randomly distributed on the metallic sites.

The thermal properties of $[Er(btc)(H_2O)_5{\cdot}3.5H_2O]_\infty$ and $[Er_2(bdc)_3(H_2O)_4]_\infty$ have already been described.[19,17] According to these studies, the anhydrous phases were thermally obtained by heating the hydrated phases in a furnace at 300 °C for 30 min. [Er(btc)] (374.377): calcd. C 28.9, H 0.8, Er 44.7, O 25.6; found C 28.8, H 1.0, O 25.5, Er 44.7. $[Er_2(bdc)_3]_\infty$ (826.867): calcd. C 34.9, H 1.5, O 23.2, Er 40.5; found C 34.5, H 1.80, Er 40.5, O 23.3. The structure type of the $(bdc)^{3-}$-containing anhydrous compound was assumed on the basis of its X-ray diffraction powder diagram.

X-ray Powder Diffraction: The diagrams were collected by using a Panalytical X′Pert Pro diffractometer with an X′celerator detector. The typical recording conditions were 40 kV, 40 mA for Cu-K_α (λ = 1.542 Å), the diagrams were recorded in θ/θ mode in 60 min between 5 and 75° (8378 measurements) with a step size of 0.0084° and a scan time of 50 s. The calculated patterns were produced by using the Powdercell and WinPLOTR software programs.[29–32] The patterns were taken as experimental data in REFLEX module of the MS Modeling Software.[33] Then, they were refined by using Rietveld refinement[34,35] with Pseudo-Voigt profile to compute refined cell parameters for each compound.

Scanning Electron Microscopy (SEM-EDS Analysis): The powder measurements of the heteropolymetallic coordination polymers were performed by using SEM. All observations and measurements were carried out with a JEOL JSM 6400 scanning electron microscopy (JEOL Ltd.Tokyo Japan) with EDS analysis system (OXFORD Link INCA). The voltage was kept at 9 kV, and the sample were mounted on carbon stubs and coated for 5 min with gold/palladium alloy using a sputter coater (Jeol JFC 1100).

Solid-State Luminescence Measurements: Excitation of the finely powdered samples was achieved at 488 nm with a Coherent Innova argon laser. For emission in the NIR, the emitted light was analyzed at 90° with a Spex 1870 single monochromator with 950 groves mm^{-1} holographic gratings blazed at 900 nm. Light intensity was measured with a NIR photomultiplier Hamamatsu H9170–75 cooled by Pelletier effect at –60 °C (range 930–1700 nm) and coupled to a Stanford Research SR400 photon counting system. Data were transferred into a PC and emission spectra were corrected for the instrumental function regularly updated. Luminescent lifetimes were determined upon excitation at 355 nm provided by a Quantum Brillant Nd:YAG laser equipped with frequency tripler. The output signal of the NIR photomultiplier was

Table 4. Chemical analysis results for $[Er_{2-2x}Y_{2x}(bdc)(H_2O)_4]_\infty$ with $0 < x < 1$.

x	MW / gmol^{-1}	Analysis calcd. (found) / %				
		Er	Y	O	C	H
0.2	867.584	30.8 (30.9)	4.1 (4.2)	29.5 (29.4)	33.2 (33.1)	2.3 (2.3)
0.5	820.571	20.4 (20.4)	10.8 (10.9)	31.2 (31.1)	35.1 (35.1)	2.5 (2.5)
0.8	773.558	8.6 (8.8)	18.4 (18.5)	33.1 (33.0)	37.3 (37.2)	2.6 (2.5)
0.9	757.887	4.4 (4.4)	21.1 (21.0)	33.8 (33.8)	38.0 (38.0)	2.7 (2.8)

Table 5. Chemical analysis results for $[Er_{2-2x}Yb_{2x}(bdc)(H_2O)_4]_\infty$ with $0 < x < 1$.

x	MW / gmol^{-1}	Analysis calcd. (found) / %				
		Er	Yb	O	C	H
0.2	901.238	29.7 (29.8)	7.7 (7.5)	28.4 (28.5)	32.0 (32.2)	2.2 (2.0)
0.5	904.706	18.5 (18.5)	19.1 (19.1)	28.3 (28.0)	31.9 (32.2)	2.2 (2.2)

fed into a Stanford Research SR-430 multichannel scaler and transferred to a PC. Lifetimes are averages of three independent determinations. Quantum yields were determined on solid samples with a Fluorolog FL3–221 spectrofluorimeter from Horiba-Jobin–Yvon-Spex at 295 K, under ligand excitation, according to an absolute method[36] using a home-modified integration sphere.[37] Each sample was measured several times under slightly different experimental conditions. The estimated error for quantum yields is 10%.

Acknowledgments

Région Bretagne is acknowledged for financial support. Pr. B. Lambert (INSA Rennes, France) and Dr. J.-L. Adam (Université de Rennes 1, France) are warmly acknowledged for fruitful discussions. The Centre de Microscopie Electronique à Balayage et micro-Analyse is acknowledged for SEM measurements. J. C. B. and F. G. thank the Swiss National Science Foundation for support.

[1] S. Comby, J. C. G. Bünzli, K. A. Gschneider, V. K. Pecharsky in *Handbook on the Physics and Chemistry of Rare Earths*, Elsevier, Amsterdam, **2007**, pp. 1–353.
[2] J. Kido, Y. Okamoto, *Chem. Rev.* **2002**, *102*, 2357–2368.
[3] K. Kuriki, Y. Koike, Y. Okamoto, *Chem. Rev.* **2002**, *102*, 2347–2356.
[4] L. Winkless, R. H. C. Tan, Y. Zheng, M. Motevalli, P. B. Wyatt, W. P. Gillin, *App. Phys. Lett.* **2006**, *89*, 111115.
[5] P. K. Sekhar, A. R. Wilkinson, R. G. Elliman, T. H. Khim, S. Bhansali, *J. Phys. Chem. C* **2008**, *112*, 20109–20113.
[6] J. L. Adam, *Chem. Rev.* **2002**, *102*, 2461–2476.
[7] G. N. van den Hoven, R. J. I. M. Koper, A. Polman, C. van Dam, J. W. M. van Uffelen, M. K. Smit, *Appl. Phys. Lett.* **1996**, *68*, 1886–1888.
[8] T. Feuchter, E. K. Mwarania, J. Wang, L. Reekie, J. S. Wilkinson, *IEEE Photonics Technology. Lett.* **1992**, *4*, 542–544.
[9] P. Becker, R. Brinkmann, M. Dinand, W. Sohler, H. Suche, *Appl. Phys. Lett.* **1992**, *61*, 1257–1259.
[10] A. C. Grimsdale, K. Leok Chan, R. E. Martin, P. G. Jokisz, A. B. Holmes, *Chem. Rev.* **2009**, *109*, 897–1091.
[11] S. V. Eliseeva, J. C. G. Bünzli, *Chem. Soc. Rev.*, in press.
[12] O. Guillou, C. Daiguebonne in *Handbook on the Physics and Chemistry of Rare Earths* (Eds.: K. A. Gschneider, J. C. G. Bünzli, V. K. Pecharsky), Elsevier, **2005**, vol. 34, pp. 359–404.
[13] J. L. Song, C. Lei, J. G. Mao, *Inorg. Chem.* **2004**, *43*, 5630–5634.
[14] Z. H. Zhang, Y. Song, T. A. Okamura, Y. Hasegawa, W. Y. Sun, N. Ueyama, *Inorg. Chem.* **2006**, *45*, 2896–2902.
[15] B. Chen, Y. Yang, F. Zapata, G. Qian, Y. Luo, J. Zhang, E. B. Lobkovsky, *Inorg. Chem.* **2006**, *45*, 8882–8886.
[16] C. Daiguebonne, O. Guillou, Y. Gérault, A. Lecerf, K. Boubekeur, *Inorg. Chim. Acta* **1999**, *284*, 139–145.
[17] C. Daiguebonne, N. Kerbellec, O. Guillou, J. C. G. Bünzli, F. Gumy, L. Catala, T. Mallah, N. Audebrand, Y. Gérault, K. Bernot, G. Calvez, *Inorg. Chem.* **2008**, *47*, 3700–3708.
[18] M. S. Wrighton, D. S. Ginley, D. L. Morse, *J. Phys. Chem.* **1974**, *78*, 2229–2233.
[19] C. Daiguebonne, O. Guillou, Y. Gérault, K. Boubekeur, *Recent. Res. Development Inorg. Chem.* **2000**, *2*, 165–183.
[20] C. Daiguebonne, O. Guillou, K. Boubekeur, *Inorg. Chim. Acta* **2000**, *304*, 161–169.
[21] C. Daiguebonne, N. Kerbellec, K. Bernot, Y. Gérault, A. Deluzet, O. Guillou, *Inorg. Chem.* **2006**, *45*, 5399–5406.
[22] N. Kerbellec, L. Catala, C. Daiguebonne, A. Gloter, O. Stephan, J. C. G. Bünzli, O. Guillou, T. Mallah, *New J. Chem.* **2008**, *32*, 584–587.
[23] D. L. Dexter, *J. Chem. Phys.* **1953**, *21*, 836–850.
[24] T. Förster, *Comparative Effects of Radiation*, Wiley, New York, **1960**.
[25] N. Kerbellec, D. Kustaryono, V. Haquin, M. Etienne, C. Daiguebonne, O. Guillou, *Inorg. Chem.* **2009**, *48*, 2837–2843.
[26] A. Deluzet, W. Maudez, C. Daiguebonne, O. Guillou, *Cryst. Growth Des.* **2003**, *3*, 475–479.
[27] A. Kornienko, T. J. Emge, G. A. Kumar, R. E. Riman, J. G. Brennan, *J. Am. Chem. Soc.* **2005**, *127*, 3501–3505.
[28] J. F. Desreux in *Lanthanide Probes in Life, Chemical and Earth Sciences* (Eds.: G. R. Choppin, J. C. G. Bünzli), Elsevier, Amsterdam, **1989**, p. 43.
[29] W. Kraus, G. Nolze, *J. Appl. Crystallography.* **1996**, *29*, 301–303.
[30] T. Roisnel, J. Rodriguez-Carjaval, *Materials Science Forum, Proceedings of the Seventh European Powder Diffraction Conference (EPDIC 7)* **2000**, p. 118–123.
[31] T. Roisnel, J. Rodriguez-Carjaval, *Mater. Sci. Forum*, Proceedings of the Seventh European Powder Diffraction Conference (EPDIC 7), **2000**, pp. 118–123.
[32] T. Roisnel, J. Rodriguez-Carjaval, *Mater. Sci. Forum* **2001**, *118*, 378.
[33] *Accelrys*, Accelrys Software Inc., **2005**.
[34] P. Thompson, D. E. Cox, J. B. Hasting, *J. Appl. Crystallography* **1987**, *20*, 79–83.
[35] H. M. Rietveld, *J. Appl. Crystallography* **1969**, *2*, 65–71.
[36] J. C. Mello, H. F. Wittmann, R. H. Friend, *Adv. Mater.* **1997**, *9*, 230–232.
[37] A. Aebisher, F. Gumy, J. C. G. Bünzli, *Phys. Chem. Chem. Phys.* **2009**, *11*, 1346–1353.
[38] The summation symbol is used here for simplifying the writing of the general chemical formula. It means that the compounds can contain between 1 and 13 different lanthanide ions, all the relative proportions being accessible.
[39] $[Er_2(bdc)_3(H_2O)_8 \cdot 6H_2O]_\infty$ crystallizes in the triclinic system, space group $P\bar{1}$ with a = 7.8373(1) Å, b = 9.5854(2) Å, c = 10.6931(2) Å, α = 68.7770(8)°, β = 70.8710(8)°, γ = 75.3330(12)° and Z = 4.

Received: June 17, 2009
Published Online: September 16, 2009

